

# Reversing the thermodynamic arrow of time using quantum correlations

Kaonan Micadei,<sup>1,\*</sup> John P. S. Peterson,<sup>2,\*</sup> Alexandre M. Souza,<sup>2</sup> Roberto S. Sarthour,<sup>2</sup> Ivan S. Oliveira,<sup>2</sup> Gabriel T. Landi,<sup>3</sup> Tiago B. Batalhão,<sup>4,5</sup> Roberto M. Serra,<sup>1,6,†</sup> and Eric Lutz<sup>7,‡</sup>

<sup>1</sup>*Centro de Ciências Naturais e Humanas, Universidade Federal do ABC, Avenida dos Estados 5001, 09210-580 Santo André, São Paulo, Brazil*

<sup>2</sup>*Centro Brasileiro de Pesquisas Físicas, Rua Dr. Xavier Sigaud 150, 22290-180 Rio de Janeiro, Rio de Janeiro, Brazil*

<sup>3</sup>*Instituto de Física, Universidade de São Paulo, C.P. 66318, 05315-970 São Paulo, SP, Brazil*

<sup>4</sup>*Singapore University of Technology and Design, 8 Somapah Road, Singapore 487372*

<sup>5</sup>*Centre for Quantum Technologies, National University of Singapore, 3 Science Drive 2, Singapore 117543*

<sup>6</sup>*Department of Physics, University of York, York YO10 5DD, United Kingdom*

<sup>7</sup>*Department of Physics, Friedrich-Alexander-Universität Erlangen-Nürnberg, 91058 Erlangen, Germany*

The second law permits the prediction of the direction of natural processes, thus defining a thermodynamic arrow of time. However, standard thermodynamics presupposes the absence of initial correlations between interacting systems. We here experimentally demonstrate the reversal of the arrow of time for two initially quantum correlated spins-1/2, prepared in local thermal states at different temperatures, employing a Nuclear Magnetic Resonance setup. We observe a spontaneous heat flow from the cold to the hot system. This process is enabled by a trade off between correlations and entropy that we quantify with information-theoretical quantities.

Irreversibility is a longstanding puzzle in physics. While microscopic laws of motion are invariant under time reversal, all macroscopic phenomena have a preferred direction in time [1, 2]. Heat, for instance, spontaneously flows from hot to cold. Eddington has called this asymmetry the *arrow of time* [3]. At the phenomenological level, the second law of thermodynamics allows one to predict which processes are possible in nature: only those with non-negative mean entropy production do occur [4]. A microscopic resolution of the apparent paradox of irreversibility was put forward by Boltzmann, when he noted that initial conditions break the time-reversal symmetry of the otherwise reversible dynamics [5]. Quantitative experimental confirmation of this conjecture has recently been obtained for a driven classical Brownian particle and for an electrical RC circuit [6], as well as for a driven quantum spin [7], and a driven quantum dot [8]. These experiments have been accompanied by a surge of theoretical studies on the classical and quantum arrows of time [9–16]. It has in particular been shown that a preferred direction of average behavior may be discerned irrespective of the size of the system [17].

In addition to breaking time reversal, initial conditions also determine the arrow's direction. The observation of the average positivity of the entropy production in nature is often explained by the low entropy value of the initial state [5]. This opens the possibility to control or even reverse the arrow of time depending on the initial conditions. In standard thermodynamics, systems are assumed to be uncorrelated before thermal contact. As a result, according to the second law heat will flow from the hot to the cold body. However, it has been theoretically suggested that for quantum correlated local thermal states, heat might flow from the cold to the hot system, thus effectively reversing the arrow's direction [9–11].

Here we report the experimental demonstration of the reversal of the arrow of time for two initially quantum correlated qubits (two spin-1/2 systems) prepared in local thermal states at different temperatures employing Nuclear Magnetic Resonance (NMR) techniques (Fig. 1A). Allowing thermal contact between the two qubits, we track the evolution of their local states with the help of quantum state tomography (QST) [18]. We experimentally determine the energy change of each spin and the variation of their mutual information [19]. For initially correlated systems, we observe a spontaneous heat current from the cold to the hot spin and show that this process is made possible by a decrease of the mutual information between the spins. The second law for the isolated two-spin system is therefore verified. However, the standard second law in its local form apparently fails to apply to this situation with initial quantum correlations. We further establish the nonclassicality of the initial correlation by evaluating its non-zero geometric quantum discord, a measure of quantumness [20, 21]. We finally theoretically derive and experimentally investigate an expression for the heat current that reveals the trade off between information and entropy.

NMR offers an exceptional degree of preparation, control, and measurement of coupled nuclear spin systems [18, 22]. It has for this reason become a premier tool for the study of quantum thermodynamics [7, 23, 24]. In our investigation, we consider two nuclear spins-1/2, in the <sup>13</sup>C and <sup>1</sup>H nuclei of a <sup>13</sup>C-labeled CHCl<sub>3</sub> liquid sample diluted in Acetone-d<sub>6</sub> (Fig. 1B). The sample is placed inside a superconducting magnet that produces a longitudinal static magnetic field (along the positive *z*-axis) and the system is manipulated by time-modulated transverse radio-frequency (rf) fields. We study processes in a time interval of few milliseconds which is much shorter

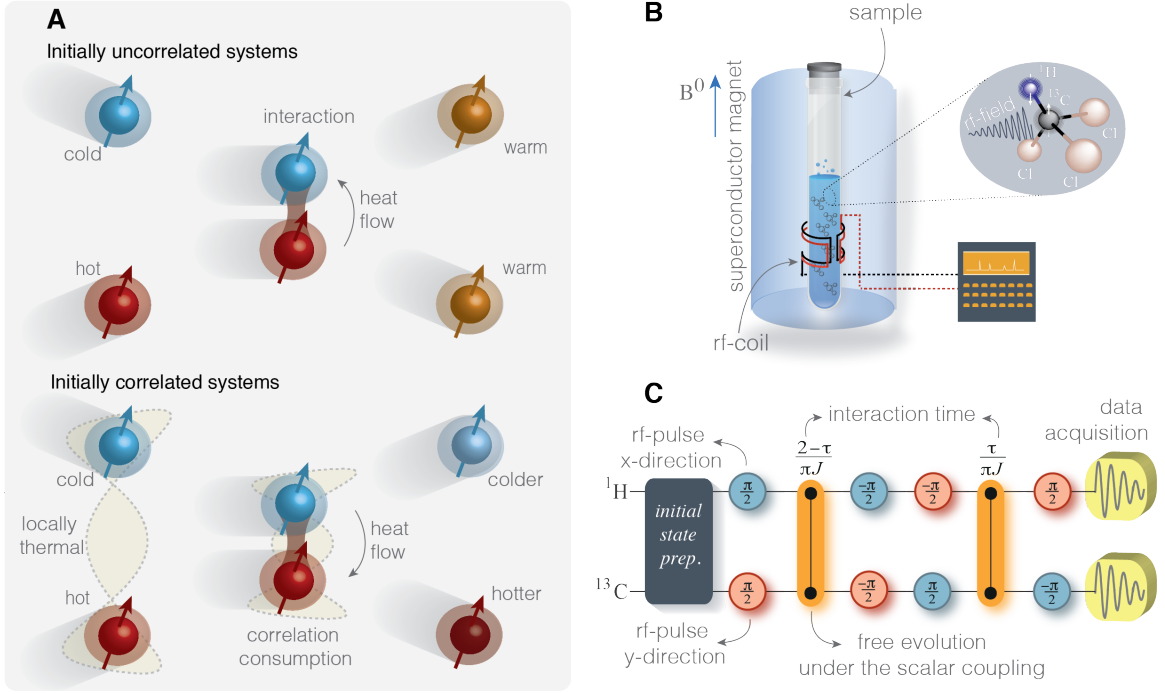


Figure 1. **Schematic of the experimental setup.** (A) Heat flows from the hot to the cold spin (at thermal contact) when both are initially uncorrelated. This corresponds to the standard thermodynamic arrow of time. For initially quantum correlated spins, heat is spontaneously transferred from the cold to the hot spin. The arrow of time is here reversed. (B) View of the magnetometer used in our NMR experiment. A superconducting magnet, producing a high intensity magnetic field ( $B_0$ ) in the longitudinal direction, is immersed in a thermally shielded vessel in liquid He, surrounded by liquid N in another vacuum separated chamber. The sample is placed at the center of the magnet within the radio frequency coil of the probe head inside a 5mm glass tube. (C) Experimental pulse sequence for the partial thermalization process. The blue (red) circle represents  $x$  ( $y$ ) rotations by the indicated angle. The orange connections represents a free evolution under the scalar coupling,  $\mathcal{H}_{J^{\text{HC}}}^{\text{HC}} = (\pi\hbar/2)J\sigma_z^{\text{H}}\sigma_z^{\text{C}}$ , between the  $^1\text{H}$  and  $^{13}\text{C}$  nuclear spins during the time indicated above the symbol. We have performed 22 samplings of the interaction time  $\tau$  in the interval 0 to 2.32 ms.

than any relevant decoherence time of the system (of the order of few seconds) [23]. The dynamics of the combined spins in the sample is thus effectively closed and the total energy is conserved to an excellent approximation. Our aim is to study the heat exchange between the  $^1\text{H}$  (system  $A$ ) and  $^{13}\text{C}$  (system  $B$ ) nuclear spins under a partial thermalization process in the presence of initial correlations. Employing a sequence of transversal rf-field and longitudinal field-gradient pulses, we prepare an initial state of both nuclear spins ( $A$  and  $B$ ) of the form,

$$\rho_{AB}^0 = \rho_A^0 \otimes \rho_B^0 + \chi_{AB}, \quad (1)$$

where  $\chi_{AB} = \alpha|01\rangle\langle 10| + \alpha^*|10\rangle\langle 01|$  is a correlation term and  $\rho_i^0 = \exp(-\beta_i\mathcal{H}_i)/\mathcal{Z}_i$  a thermal state at inverse temperature  $\beta_i = 1/(k_B T_i)$ ,  $i = (A, B)$ , with  $k_B$  the Boltzmann constant. The state  $|0\rangle$  ( $|1\rangle$ ) represents the ground (excited) eigenstate of the Hamiltonian  $\mathcal{H}_i$ , and  $\mathcal{Z}_i = \text{Tr}_i \exp(-\beta_i\mathcal{H}_i)$  is the partition function. The individual nuclear spin Hamiltonian, in a double-rotating frame with the nuclear spins ( $^1\text{H}$  and  $^{13}\text{C}$ ) Larmor frequency [25], may be written as  $\mathcal{H}_i = h\nu_0(\mathbf{1} - \sigma_z^i)/2$ , with  $\nu_0 = 1$  kHz effectively determined by a nuclei rf-field offset. In Eq. (1), the coupling strength should

satisfy  $|\alpha| \leq \exp[-h\nu_0(\beta_A + \beta_B)/2]/(\mathcal{Z}_A\mathcal{Z}_B)$  to ensure positivity. We consider two distinct cases: for  $\alpha = 0$  the two spins are initially uncorrelated as assumed in standard thermodynamics, while for  $\alpha \neq 0$  the joint state is initially correlated. We note that since  $\text{Tr}_i \chi_{AB} = 0$ , the two spin states are locally thermal in both situations. A partial thermalization between the qubits is described by the effective (Dzyaloshinskii-Moriya) interaction Hamiltonian,  $\mathcal{H}_{AB}^{\text{eff}} = (\pi\hbar/2)J(\sigma_x^A\sigma_y^B - \sigma_y^A\sigma_x^B)$ , with  $J = 215.1$  Hz [26, 27]. We implement the corresponding evolution operator,  $\mathcal{U}_\tau = \exp(-i\tau\mathcal{H}_{AB}^{\text{eff}}/\hbar)$ , by combining free evolutions under the natural hydrogen-carbon scalar coupling and rf-field rotations (Fig. 1C).

Since no work is performed, the heat absorbed by one qubit is given by its internal energy variation along the dynamics,  $Q_i = \Delta E_i$ , where  $E_i = \text{Tr}_i \rho_i \mathcal{H}_i$  is the  $z$ -component of the nuclear spin magnetization. For the combined system, the two heat contributions satisfy the inequality [9–11],

$$\beta_A Q_A + \beta_B Q_B \geq \Delta I(A:B), \quad (2)$$

where  $\Delta I(A:B)$  is the change of mutual information

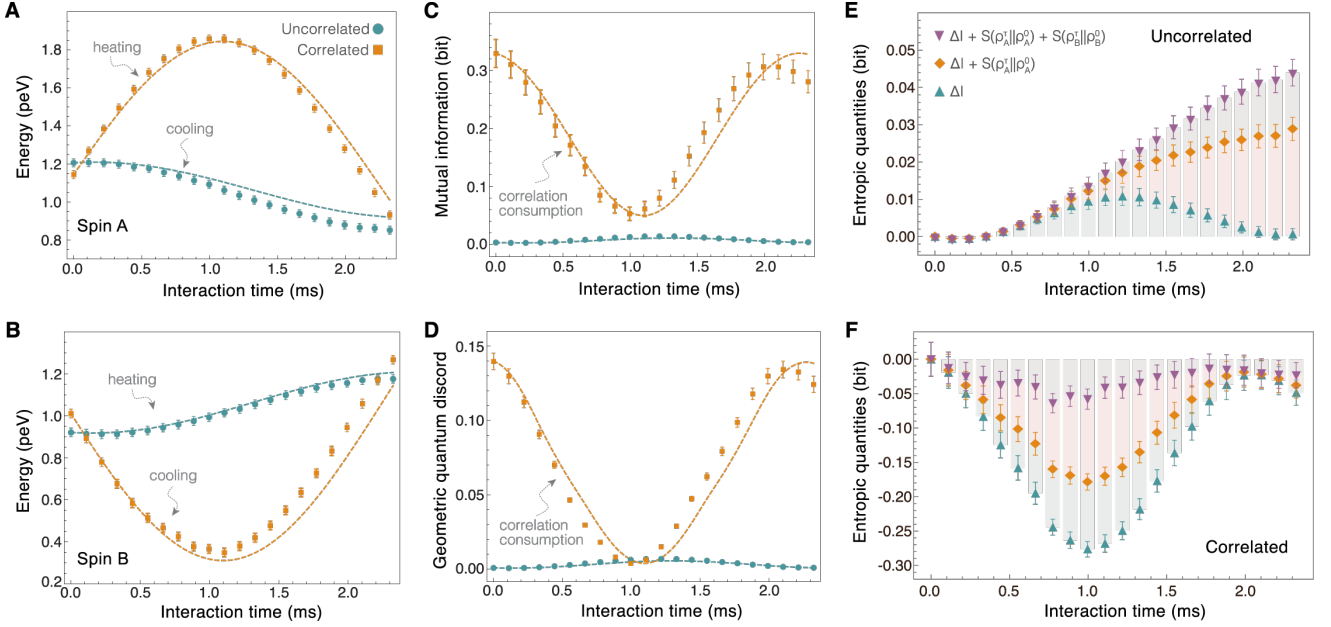


Figure 2. **Dynamics of heat, correlations, and entropic quantities.** (A) Internal energy of qubit  $A$  along the partial thermalization process. (B) Internal energy of qubit  $B$ . In the absence of initial correlations, the hot qubit  $A$  cools down and the cold qubit  $B$  heats up (cyan circles in panel A and B). By contrast, in the presence of initial quantum correlations, the heat current is reversed as the hot qubit  $A$  gains and the cold qubit  $B$  loses energy (orange squares in panel A and B). This reversal is made possible by a decrease of the mutual information (C) and of the geometric quantum discord (D). Different entropic contributions to the heat current (5) in the uncorrelated (E) and correlated (F) case. Reversal occurs when the negative variation of the mutual information,  $\Delta I(A:B)$ , compensates the positive entropy productions,  $S(\rho_A^\tau || \rho_A)$  and  $S(\rho_B^\tau || \rho_B)$ , of the respective qubits. The symbols represent experimental data and the dashed lines are numerical simulations.

between  $A$  and  $B$ . The mutual information, defined as  $I(A:B) = S_A + S_B - S_{AB} \geq 0$ , is a measure of the total correlations between two systems [19], where  $S_i = -\text{Tr}_i \rho_i \ln \rho_i$  is the von Neumann entropy of state  $\rho_i$ . For initially uncorrelated spins, the initial mutual information is zero. As a result, it can only increase during thermalization,  $\Delta I(A:B) \geq 0$ . Noting that  $Q_A + Q_B = 0$  for the isolated bipartite system, we find [9–11],

$$Q_B(\beta_B - \beta_A) \geq 0 \quad (\text{uncorrelated}). \quad (3)$$

Heat hence flows from the hot to the cold spin,  $Q_B > 0$  if  $T_A \geq T_B$ . This is the standard arrow of time. By contrast, for initially correlated qubits, the mutual information may decrease during the thermal contact between the spins. In that situation, we may have [9–11],

$$Q_B(\beta_B - \beta_A) \leq 0 \quad (\text{correlated}). \quad (4)$$

Heat flows in this case from the cold to the hot qubit: the arrow of time is reversed. We quantitatively characterize the occurrence of such reversal by computing the heat current at any time  $\tau$ , obtaining [25],

$$\Delta \beta Q_B = \Delta I(A:B) + S(\rho_A^\tau || \rho_A) + S(\rho_B^\tau || \rho_B), \quad (5)$$

where  $\Delta \beta = \beta_B - \beta_A \geq 0$  and  $S(\rho_i^\tau || \rho_i) = \text{Tr}_i \rho_i^\tau (\ln \rho_i^\tau - \ln \rho_i) \geq 0$  denotes the relative entropy [19] between the

evolved  $\rho_{A(B)}^\tau = \text{Tr}_{B(A)} \mathcal{U}_\tau \rho_{AB}^0 \mathcal{U}_\tau^\dagger$  and the initial  $\rho_{A(B)}^0$  reduced states. The latter quantifies the entropic distance between the state at time  $\tau$  and the initial thermal state describing also the entropy produced during the thermalization process [28, 29]. According to Eq. (5), the direction of the arrow is therefore reversed whenever the decrease of mutual information compensates the entropy production. The fact that initial correlations may be used to decrease entropy has first been emphasized by Lloyd [30] and further investigated in Refs. [31, 32].

In our experiment, we prepare the two-qubit system in an initial state of the form (1) with effective spin temperatures  $\beta_A^{-1} = 4.66 \pm 0.13$  peV ( $\beta_A^{-1} = 4.30 \pm 0.11$  peV) and  $\beta_B^{-1} = 3.31 \pm 0.08$  peV ( $\beta_B^{-1} = 3.66 \pm 0.09$  peV) for the uncorrelated (correlated) case  $\alpha = 0.00 \pm 0.01$  ( $\alpha = -0.19 \pm 0.01$ ) [25]. In order to quantify the quantumness of the initial correlation in the latter case, we consider the normalized geometric discord, defined as  $D_g = \min_{\psi \in \mathcal{C}} 2 \|\rho - \psi\|^2$  where  $\mathcal{C}$  is the set of all states classically correlated [20, 21]. The geometric discord for two qubits can be directly evaluated from the measured QST data [25]. We find the nonzero value  $D_g = 0.14 \pm 0.01$  for the initially correlated state prepared in the experiment.

We use the experimentally reconstructed density operators of both qubits to evaluate the changes of their in-

ternal energies, mutual information, and geometric quantum discord during thermal contact (Figs. 2, A to F). We observe the standard arrow of time in the absence of initial correlations ( $\alpha \simeq 0$ ), i.e., the hot qubit  $A$  cools down,  $Q_A < 0$ , while the cold qubit  $B$  heats up,  $Q_B > 0$  (circles symbols in Figs. 2, A and B). At the same time, the mutual information and the geometric quantum discord increase, as correlations build up following the thermal interaction (circles symbols in Figs. 2, C and D). The situation changes dramatically in the presence of initial quantum correlations ( $\alpha \neq 0$ ): the arrow of time is here reversed in the time interval,  $0 < \tau < 2.1$  ms, as heat flows from the cold to the hot spin,  $Q_A = -Q_B > 0$  (squares symbols in Figs. 2, A and B). This reversal is accompanied by a decrease of mutual information and geometric quantum discord (squares symbols in Fig. 2, C and D). In this case, quantum correlations are converted into energy and used to switch the direction of the heat flow, in an apparent violation of the second law. Correlations reach their minimum at around  $\tau \approx 1.05$  ms, after which they build up again. Once they have passed their initial value at  $\tau \approx 2.1$  ms, energy is transferred in the expected direction, from hot to cold. In all cases, we obtain good agreement between experimental data (symbols) and theoretical simulations (dashed lines). Small discrepancies seen as time increases are mainly due to inhomogeneities in the control fields.

The experimental investigation of Eq. (5) as a function of the thermalization time is presented in Fig. 2, E and F. While the relative entropies steadily grow in the absence of initial correlations, they exhibit an increase up to 1.05 ms followed by a decrease in presence of initial correlations. The latter behavior reflects the pattern of the qubits already seen in Fig. 2, A and B, for the average energies. We note in addition a positive variation of the mutual information in the uncorrelated case and a large negative variation in the correlated case. The latter offsets the increase of the relative entropies and enables the reversal of the heat current. These findings provide direct experimental evidence for the trading of quantum mutual information and entropy production.

By revealing the fundamental influence of initial quantum correlations on time's arrow, our experiment highlights the subtle interplay of quantum mechanics, thermodynamics and information theory. It further emphasizes the limitations of the standard local formulation of the second law for initially correlated systems and offers at the same time a novel mechanism to control heat on the microscale. It additionally establishes that the arrow of time is not an absolute but a relative concept that depends on the choice of initial conditions. While we have observed reversal of the arrow for the case of two spins, numerical simulations show that reversals may also occur for a spin interacting with larger spin environments [25]. Thus, an anomalous heat current does not seem to be restricted to extremely microscopic systems. The

precise scaling of this effect with the system size is an interesting subject for future experimental and theoretical investigations. Our results on the thermodynamic arrow of time might also have stimulating consequences on the cosmological arrow of time [30].

*Acknowledgments.* We acknowledge financial support from UFABC, CNPq, CAPES, FAPERJ, and FAPESP. R.M.S. gratefully acknowledges financial support from the Royal Society through the Newton Advanced Fellowship scheme (Grant no. NA140436). K.M. acknowledges the hospitality of Friedrich-Alexander-Universität Erlangen-Nürnberg, and CAPES and DAAD for financial support. This research was performed as part of the Brazilian National Institute of Science and Technology for Quantum Information (INCT-IQ).

---

\* These authors contributed equally to this work.

† serra@ufabc.edu.br

‡ eric.lutz@fau.de

- [1] J. L. Lebowitz, Boltzmann's entropy and time's arrow. *Physics today* **46**, 32 (1993).
- [2] H. D. Zeh, *The Physical Basis of the Direction of Time* (Springer, 2007).
- [3] A. S. Eddington, *The Nature of the Physical World* (Macmillan, 1928).
- [4] H. B. Callen, *Thermodynamics and an Introduction to Thermostatistics* (Wiley, ed. 2, 1985).
- [5] Boltzmann L. , Ann. Phys. (Leipzig) **57** (1896) 773; Sitzungsberichte Akad. Wiss., Vienna, part II, **75** (1877) 67 (translated and reprinted in: S.G. Brush, Kinetic Theory 2, (Pergamon, Oxford, 1966) pp. 218, 188).
- [6] D. Andrieux, P. Gaspard, S. Ciliberto, N. Garnier, S. Joubaud, A. Petrosyan, Entropy production and time asymmetry in nonequilibrium fluctuations. *Phys. Rev. Lett.* **98**, 150601 (2007).
- [7] T. B. Batalhão, A. M. Souza, R. S. Sarthour, I. S. Oliveira, M. Paternostro, E. Lutz, R. M. Serra, Irreversibility and the arrow of time in a quenched quantum system. *Phys. Rev. Lett.* **115**, 190601 (2015).
- [8] A. Hofmann, V. F. Maisi, J. Basset, C. Reichl, W. Wegscheider, T. Ihn, K. Ensslin, C. Jarzynski, Heat dissipation and fluctuations in a driven quantum dot. *Phys. Status Solidi B* **254**, 1600546 (2017).
- [9] M. H. Partovi, Entanglement versus stosszahlansatz: disappearance of the thermodynamic arrow in a high-correlation environment. *Phys. Rev. E* **77**, 021110 (2008).
- [10] D. Jennings, T. Rudolph, Entanglement and the thermodynamic arrow of time. *Phys. Rev. E* **81**, 061130 (2010).
- [11] S. Jevtic, D. Jennings, T. Rudolph, Maximally and minimally correlated states attainable within a closed evolving system. *Phys. Rev. Lett.* **108**, 110403 (2012).
- [12] L. Maccone, Quantum solution to the arrow-of-time dilemma. *Phys. Rev. Lett.* **103**, 080401 (2009).
- [13] J. M. R. Parrondo, C. V. den Broeck, R. Kawai, Entropy production and the arrow of time. *New J. Phys.* **11**, 073008 (2009).
- [14] C. Jarzynski, Equalities and inequalities: irreversibility and the second law of thermodynamics at the nanoscale.

- Annu. Rev. Condens. Matter Phys.* **2**, 329–351 (2011).
- [15] É. Roldán, I. Neri, M. Dörpinghaus, H. Meyr, and Frank Jülicher, Decision Making in the Arrow of Time. *Phys. Rev. Lett.* **115**, 250602 (2015).
- [16] V. Vedral, The arrow of time and correlations in quantum physics. <https://arxiv.org/abs/1605.00926> (2016).
- [17] M. Campisi, P. Hänggi, Fluctuation, dissipation and the arrow of time. *Entropy* **13**, 2024 (2011).
- [18] I. Oliveira, R. Sarthour, T. Bonagamba, E. Azevedo, J. C. C. Freitas, *NMR Quantum Information Processing* (Elsevier, 2007).
- [19] M. A. Nielsen, I. L. Chuang, *Quantum Computation and Quantum Information* (Cambridge, 2010).
- [20] B. Dakić, V. Vedral, Č. Brukner, Necessary and sufficient condition for nonzero quantum discord. *Phys. Rev. Lett.* **105**, 190502 (2010).
- [21] D. Girolami, G. Adesso, Observable measure of bipartite quantum correlations. *Phys. Rev. Lett.* **108**, 150403 (2012).
- [22] L. M. K. Vandersypen, I. L. Chuang, NMR techniques for quantum control and computation. *Rev. Mod. Phys.* **76**, 1037–1069 (2005).
- [23] T. B. Batalhão, A. M. Souza, L. Mazzola, R. Auccaise, R. S. Sarthour, I. S. Oliveira, J. Goold, G. De Chiara, M. Paternostro, R. M. Serra, Experimental reconstruction of work distribution and study of fluctuation relations in a closed quantum system. *Phys. Rev. Lett.* **113**, 140601 (2014).
- [24] P. A. Camati, J. P. S. Peterson, T. B. Batalhão, K. Micadei, A. M. Souza, R. S. Sarthour, I. S. Oliveira, R. M. Serra, Experimental rectification of entropy production by Maxwell’s demon in a quantum system. *Phys. Rev. Lett.* **117**, 240502 (2016).
- [25] See supplementary material.
- [26] V. Scarani, M. Ziman, P. Štelmachovič, N. Gisin, V. Bužek, Thermalizing quantum machines: dissipation and entanglement. *Phys. Rev. Lett.* **88**, 097905 (2002).
- [27] M. Ziman, P. Štelmachovič, V. Bužek, M. Hillery, V. Scarani, N. Gisin, Diluting quantum information: an analysis of information transfer in system-reservoir interactions. *Phys. Rev. A* **65**, 042105 (2002).
- [28] S. Deffner, E. Lutz, Generalized Clausius inequality for nonequilibrium quantum processes. *Phys. Rev. Lett.* **105**, 170402 (2010).
- [29] S. Deffner, E. Lutz, Nonequilibrium entropy production for open quantum systems. *Phys. Rev. Lett.* **107**, 140404 (2011).
- [30] S. Lloyd, Use of mutual information to decrease entropy: implications for the second law of thermodynamics. *Phys. Rev. A* **39**, 5378 (1989).
- [31] T. Sagawa, M. Ueda, Fluctuation theorem with information exchange: role of correlations in stochastic thermodynamics. *Phys. Rev. Lett.* **109**, 180602 (2012).
- [32] J. V. Koski, V. F. Maisi, T. Sagawa, J. P. Pekola, Experimental observation of the role of mutual information in the nonequilibrium dynamics of a Maxwell demon. *Phys. Rev. Lett.* **113**, 030601 (2014).
- [33] M. Piani, Problem with geometric discord. *Phys. Rev. A* **86**, 034101 (2012).
- [34] X. Hu, H. Fan, D. L. Zhou, W.-M. Liu, Quantum correlating power of local quantum channels. *Phys. Rev. A* **87**, 032340 (2013).
- [35] G. Benenti, G. M. Palma, Reversible and irreversible dynamics of a qubit interacting with a small environment. *Phys. Rev. A* **75**, 052110 (2007).
- [36] A. Demers, D. Greene, C. Hauser, W. Irish, J. Larson, S. Shenker, H. Sturgis, D. Swinehart, D. Terry, paper presented at the Proceedings of the Sixth Annual ACM Symposium on Principles of Distributed Computing, (Vancouver, Canada, 1987).
- [37] M. Siomau, Gossip algorithms in quantum networks, *Physics Letters A* **381**, 136 (2016).

## SUPPLEMENTARY MATERIAL

In what follows we present additional discussions, besides some theoretical and experimental details concerning the results in the main text.

**Heat current between initially correlated systems.** Here we derive the microscopic expression, displayed in Eq. (5) of the main text, for the heat flow between initially correlated systems  $A$  and  $B$ . For an initial thermal state  $\rho_i^0 = \exp(-\beta_i \mathcal{H}_i) / \mathcal{Z}_i$ , ( $i = A, B$ ), the relative entropy between the evolved  $\rho_{A(B)}^\tau = \text{Tr}_{B(A)} \mathcal{U}_\tau \rho_{AB}^0 \mathcal{U}_\tau^\dagger$  and the initial  $\rho_i^0$  marginal states reads,

$$S(\rho_i^\tau \| \rho_i^0) = -S(\rho_i^\tau) + \beta_i \text{Tr}_i(\rho_i^\tau \mathcal{H}_i) + \ln \mathcal{Z}_i, \quad (\text{S1})$$

where  $S(\rho_i^\tau)$  is the von Neumann entropy of the state  $\rho_i^\tau$ . Noting that as  $S(\rho_i^0 \| \rho_i^0) = 0$ , one can write,

$$S(\rho_i^\tau \| \rho_i^0) = S(\rho_i^\tau) - S(\rho_i^0) = -\Delta S_i + \beta_i \Delta E_i, \quad (\text{S2})$$

with the variation in the von Neumann entropy, given by  $\Delta S_i = S(\rho_i^\tau) - S(\rho_i^0)$  and the internal energy change of the  $i$ -th subsystem defined as  $\Delta E_i = \text{Tr}_i \rho_i^\tau \mathcal{H}_i - \text{Tr}_i \rho_i^0 \mathcal{H}_i$ . Energy conservation for the combined isolated system ( $AB$ ) further implies that  $\Delta E_A = -\Delta E_B = Q_B$ , for vanishing interaction energy. As a result, we obtain,

$$Q_B \Delta\beta = \Delta I(A:B) + S(\rho_A^\tau \| \rho_A^0) + S(\rho_B^\tau \| \rho_B^0), \quad (\text{S3})$$

where  $\Delta\beta = \beta_A - \beta_B$  is the inverse temperature difference and  $\Delta S_A + \Delta S_B = \Delta I(A:B)$  holds since the combined system ( $AB$ ) is isolated.

**Experimental setup.** The liquid sample consist of 50 mg of 99%  $^{13}\text{C}$ -labeled  $\text{CHCl}_3$  (Chloroform) diluted in 0.7 ml of 99.9% deuterated Acetone- $d_6$ , in a flame sealed Wildmad LabGlass 5 mm tube. Experiments were carried out in a Varian 500 MHz Spectrometer employing a double-resonance probe-head equipped with a magnetic field gradient coil. The sample is very diluted such that the intermolecular interaction can be neglected, in this way the sample can be regarded as a set of identically prepared pairs of spin-1/2 systems. The superconducting magnet (illustrated in Fig. 1B of the main text) inside of the magnetometer produces a strong intensity longitudinal static magnetic field (whose direction is taken to be along the positive  $z$  axes),  $B_0 \approx 11.75$  T. Under this filed the  $^1\text{H}$  and  $^{13}\text{C}$  Larmor frequencies are about 500 MHz and 125 MHz, respectively. The state of the

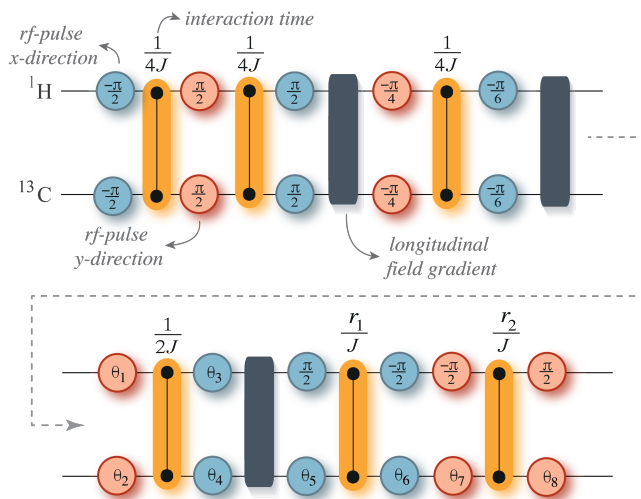


Figure S1. **Pulse sequence for the initial state preparation.** The blue (red) circle represents  $x$  ( $y$ ) local rotations by the indicated angle. Such rotations are produced by a transverse rf-field resonant with  $^1\text{H}$  or the  $^{13}\text{C}$  nuclei, with phase, amplitude, and time duration suitably adjusted. The orange connections represents a free evolution under the scalar coupling,  $\mathcal{H}_J^{\text{HC}} = (\pi\hbar/2)J\sigma_z^{\text{H}}\sigma_z^{\text{C}}$  ( $J = 215.1$  Hz), between the  $^1\text{H}$  and  $^{13}\text{C}$  nuclear spins along the time indicated above the symbol. The time modulation and intensity of the gradient pulse, the angles  $\{\theta_1, \dots, \theta_8\}$ , and the parametrized interaction times,  $r_1$  and  $r_2$ , are optimized to build an initial state equivalent to the one described in Eq. (1) of the main text.

nuclear spins are controlled by time-modulated rf-field pulses in the transverse ( $x$  and  $y$ ) direction and longitudinal field gradients.

Spin-lattice relaxation times, measured by the inversion recovery pulse sequence, are  $(\mathcal{T}_1^{\text{H}}, \mathcal{T}_1^{\text{C}}) = (7.42, 11.31)$  s. Transverse relaxations, obtained by the Carr-Purcell-Meiboom-Gill (CPMG) pulse sequence, have characteristic times  $(\mathcal{T}_2^{\text{H}}, \mathcal{T}_2^{\text{C}}) = (1.11, 0.30)$  s. The total experimental running time, to implement the partial spin thermalization, is about 2.32 ms, which is considerably smaller than the spin-lattice relaxation and therefore decoherence can be disregarded.

The initial state of the nuclear spins is prepared by spatial average techniques [7, 18, 23], being the  $^1\text{H}$  and  $^{13}\text{C}$  nuclei prepared in local pseudo-thermal states with the populations (in the energy basis of  $\mathcal{H}_0^{\text{H}}$  and  $\mathcal{H}_0^{\text{C}}$ ) and corresponding local spin temperatures displayed in Tab. SI. The initial correlated state is prepared through the pulse sequence depicted in Fig. S1.

**Error analysis.** The main sources of error in the experiments are small non-homogeneities of the transverse rf-field, non-idealities in its time modulation, and non-idealities in the longitudinal field gradient. In order to estimate the error propagation, we have used a Monte Carlo method, to sample deviations of the quantum state tomography (QST) data with a Gaussian dis-

tribution having widths determined by the variances corresponding to such data. The standard deviation of the distribution of values for the relevant information quantities is estimated from this sampling. The variances of the tomographic data are obtained by preparing the same state one hundred times, taking the full state tomography and comparing it with the theoretical expectation. These variances include random and systematic errors in both state preparation and data acquisition by QST. The error in each element of the density matrix estimated from this analysis is about 1%. All parameters in the experimental implementation, such as pulses intensity and its time duration, are optimized in order to minimize errors.

**Geometric quantum discord.** In order to quantify the quantumness of the initial correlation in the joint nuclear spin state, we use the geometric quantum discord [20, 21]. The latter provides a useful way to quantify nonclassicality of composed system in a general fashion. A general two-qubit state  $\rho$  can be written in the Bloch representation as,

$$\rho = \frac{1}{4} \left( \mathbf{1} + \sum_{j=1}^3 x_j \sigma_j \otimes \mathbf{1} + \sum_{j=1}^3 y_j \mathbf{1} \otimes \sigma_j + \sum_{j,k=1}^3 V_{jk} \sigma_j \otimes \sigma_k \right), \quad (\text{S4})$$

where  $\{\sigma_j\}$  are the Pauli matrices. The closed form expression of the geometrical quantum discord for a general two-qubit state is given by [20, 21]

$$D_g(\rho) = 2(\text{Tr} \Lambda - \lambda_{\max}), \quad (\text{S5})$$

where  $\Lambda = (\vec{x}\vec{x}^T + VV^T)/4$  and  $\lambda_{\max}$  is the largest eigenvalue of  $\Lambda$ . We have evaluated Eq. (S5) using the experimentally reconstructed qubit density operators. Note that the criticisms, concerning the geometrical quantum discord, put forward in Refs. [33, 34] do not apply to our case, since our two-qubit system is isolated. There is hence no third party that could apply a general reversible trace-preserving map on one of the spins that could alter the value of the quantum geometric discord.

**General initial correlations.** In the main text, we have considered the correlation term,  $\chi_{AB} = \alpha|01\rangle\langle 10| + \alpha^*|10\rangle\langle 01|$ , in Eq. (5) of the main text, with  $\alpha \in \mathbb{R}$ , such that it does not commute with the thermalization Hamiltonian,  $\mathcal{H}_{AB}^{\text{eff}} = (\pi\hbar/2)J(\sigma_x^A\sigma_y^B - \sigma_y^A\sigma_x^B)$ ,  $[\chi_{AB}, \mathcal{H}_{AB}^{\text{eff}}] \neq 0$ . Now, let us consider a more general choice for the amplitude of the correlation term,  $\alpha = |\alpha|e^{i\varphi}$  with the complex phase  $\varphi$ . In this case we note that  $\chi_{AB}$  does not commute with  $\mathcal{H}_{AB}^{\text{eff}}$  for  $\varphi \neq \pm\pi/2$ . In all these cases, reversals of the arrow of time do occur. However, the commutator vanishes for the particular value  $\varphi = \pm\pi/2$ . In this specific instance only the uncorrelated part of the initial state,  $\rho_A^0 \otimes \rho_B^0$ , is involved in the energy transfer induced by the thermalization Hamiltonian. As a result, the initial correlations are thermodynamically inaccessible and no reversal appears, as seen in the experimental data shown in Fig. S2. So,  $[\chi_{AB}, \mathcal{H}_{AB}^{\text{eff}}] \neq 0$  is a necessary condition to observe reversals of the heat current.

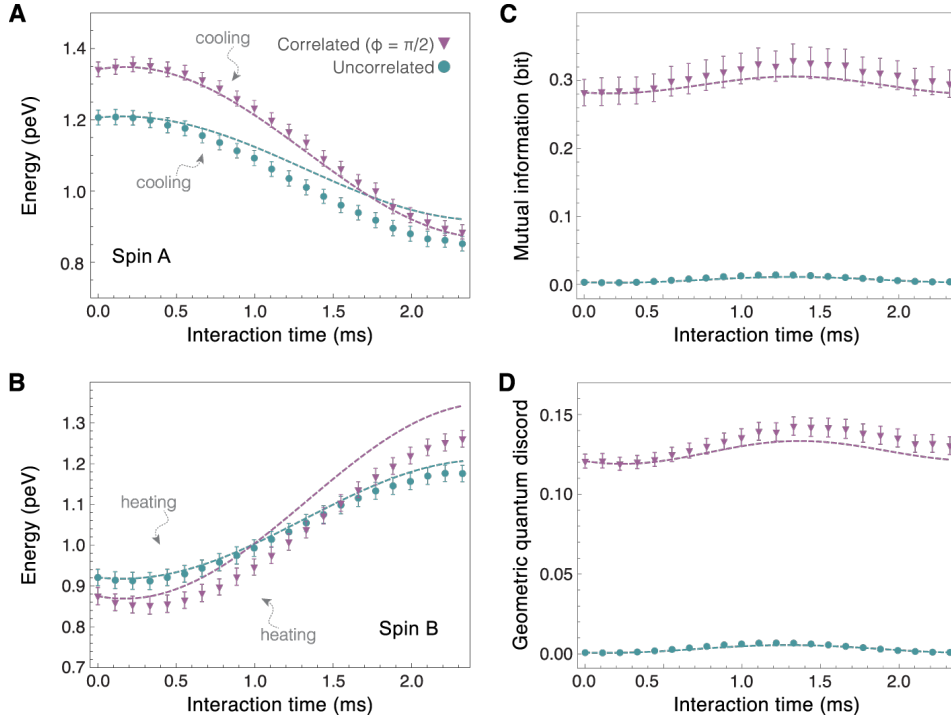


Figure S2. **Dynamics of heat and quantum correlations.** In the absence of initial correlations, the hot qubit  $A$  cools down (A) and the cold qubit  $B$  heats up (B). In the presence of initial quantum correlations that commute with the thermalization Hamiltonian,  $[\chi_{AB}, \mathcal{H}_{AB}^{eff}] = 0$ , the heat current is not reversed: the initial mutual information (C) and the geometric quantum discord (D) are not accessible to be consumed by the thermal interaction. Symbols represent experimental data and lines are numerical simulations.

Table SI. **Population and local spin-temperatures of the Hydrogen and Carbon reduced initial states.** The initial population of the nuclear spin excited state is displayed in the energy eigenbasis,  $p_{A(B)}(1) = \text{Tr}_{B(A)}(\rho_{AB}^0|1\rangle\langle 1|)$ . It is important to note again that the reduced initial state of the Hydrogen and Carbon nuclei,  $\rho_i^0$ , are diagonal in the energy basis of  $\mathcal{H}_0^H$  and  $\mathcal{H}_0^C$ , irrespective of the presence or not of the initial correlation term  $\chi_{AB}$ .

Initial state	$p_A(1)$	$p_B(1)$	$\Re(\alpha)$	$\Im(\alpha)$	$\beta_A^{-1}$ (peV)	$\beta_B^{-1}$ (peV)
Uncorrelated	$0.29 \pm 0.01$	$0.22 \pm 0.01$	$0.00 \pm 0.01$	$-0.01 \pm 0.01$	$4.70 \pm 0.13$	$3.30 \pm 0.07$
Correlated ( $\varphi \simeq \pi$ )	$0.28 \pm 0.01$	$0.24 \pm 0.01$	$-0.19 \pm 0.01$	$0.00 \pm 0.01$	$4.30 \pm 0.11$	$3.70 \pm 0.09$
Correlated ( $\varphi \simeq -\pi/2$ )	$0.32 \pm 0.01$	$0.21 \pm 0.01$	$-0.01 \pm 0.01$	$-0.17 \pm 0.01$	$5.60 \pm 0.18$	$3.10 \pm 0.07$

**Reversal of the arrow of time in a larger environment.** Different thermalization processes for a spin interacting with a multi-spin environment with random qubit-qubit collisions have been theoretically investigated [26, 27, 35]. References [26, 27] have, for instance, established equilibration induced by individual collisions with an ensemble of  $N$  spins, while Ref. [35] has focused on the relaxation generated by repeated collisions with an ensemble of two spins. Here we will consider, from a theoretical simulation perspective, a few particle scenario, where each spin, either from the system or the environment, may interact with any other spin, much like molecules in a gas. We have concretely considered a system qubit in an initial state (at hot temperature),  $\rho_0 = \exp(-\beta_{hot}\mathcal{H}_0)/\mathcal{Z}_0$ , with  $(\beta_{hot})^{-1} = 4.881$  (peV), individual nuclear spin Hamiltonian,  $\mathcal{H}_i = h\nu(\mathbf{1} - \sigma_Z^{(i)})/2$ ,

and  $\nu = 1$  kHz as in the main text. The system qubit randomly interacts with  $N$  bath qubits, a bit colder, each one initially in the state  $\rho_n = \exp(-\beta_{cold}\mathcal{H}_n)/\mathcal{Z}_n$ , with  $(\beta_{cold})^{-1} = 2.983$  (peV), the same individual nuclear spin Hamiltonian  $\mathcal{H}_n = \mathcal{H}_0$ , and  $n = 1, 2, \dots, N$ . The initial state was chosen such that the reduced bipartite density operator for the qubits 0 and 1 reads  $\rho_{01} = \text{Tr}_{rest} \rho_{total} = \rho_0 \otimes \rho_1 + \alpha(|01\rangle\langle 10| + |10\rangle\langle 01|)_{01}$  and all the eigenvalues of the total density operator  $\rho_{total}$  are positive. Here,  $\text{Tr}_{rest}$  denotes the trace over all the remaining spins except spin 0 and 1. The latter expression is a direct generalization of the two-qubit case experimentally investigated in the main text. The random spin-spin collision operator was taken of the form  $U_\lambda = \exp[\lambda(|01\rangle\langle 10| - |10\rangle\langle 01|)]$  [26, 27, 35] where  $|01\rangle\langle 10|$  act on the randomly chosen  $(j, k)$  spin pair and the inter-

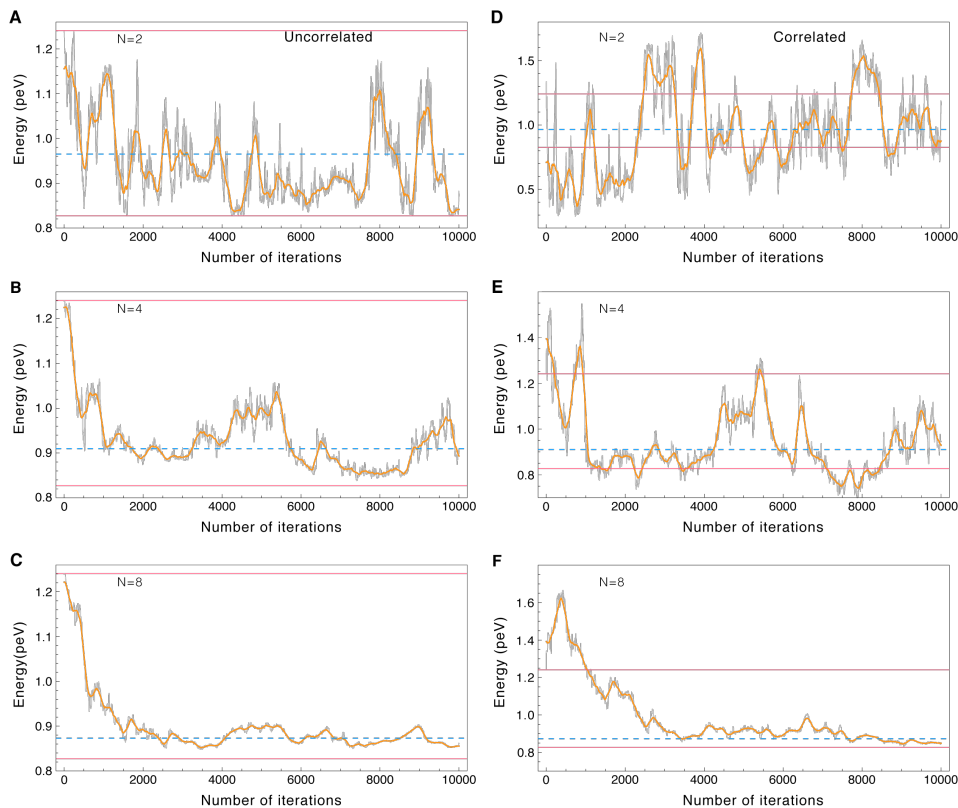


Figure S3. **Numerical simulations for larger spin environments.** Average energy of a system qubit interacting with an ensemble of  $N = 2, 4, 8$  bath qubits without initial correlations (**ABC**) and with initial correlations (**DEF**) (grey lines). In both situations, the system qubit thermalizes to a steady state, corresponding to the average energy over all the spins, as  $N$  increases (blue dashed line). In the absence of initial quantum correlations, the mean energy of the system qubit is bounded by the initial mean energies of the hot system qubit and a cold bath qubit (red solid lines). This corresponds to the standard arrow of time. However, in the presence of initial quantum correlations, the mean energy of the system qubit is seen to cross the red lines. The arrow of time is here reversed as heat flows for a cold to a hot qubit. These reversals persist even for larger environments at least for short time dynamics.

action parameter satisfies,  $|\lambda| \ll 1$ . We have performed extensive numerical simulations using a so-called gossip (or epidemic) algorithm [36] that consists basically of the following general steps (described here as a pseudo-code):

- 1: Define a number  $s$  of steps
- 2: **for each** element in  $\{1, \dots, s\}$
- 3:     Choose randomly a pair  $(j, k)$  of qubits
- 4:     Choose randomly a value for  $\lambda$  with a Gaussian distribution  $\mathcal{N}(0, \pi/50)$
- 5:     Interact the qubits  $j$  and  $k$  using  $U_\lambda$
- 6: **end for**

Such algorithm is used to spread information in a non-structured quantum network in order to make that all nodes store the same information [37]. The information we are here interested to spreading is the average individual qubit state  $\bar{\rho}_l$  with energy equal to the total energy divided by the number of qubits, corresponding to the thermalized steady state. After a sufficient large number of simulation steps, we expect that all individual qubit states will be close to the average state  $\bar{\rho}$ .

The results for the number of steps  $s = 10^4$  and sys-

tem sizes  $N = 2, 4, 8$  are shown in Fig. S3 for the uncorrelated ( $\alpha = 0$ ) and the correlated ( $\alpha = \sqrt{0.0336}$ ) cases. For each value of  $N$ , we have used the same seed for the pseudo-random number generator, so that each pair of correlated-uncorrelated simulations compares two systems under the same discrete evolution history. The grey lines represent the simulated mean energy of the system spin as a function of the number of simulation steps. Since the simulations are rather noisy (especially for small  $N$ ), we have added a smoothed orange line for better visualization of the results. The dashed blue line corresponds to the total average energy. We observe in both cases that the mean system spin energy asymptotically relaxes to the total average energy as  $N$  increases, as expected. The red solid lines (in Fig. S3) indicate the respective average initial energies of the (hot) system spin  $\rho_0$  and of the (cold) bath spins  $\rho_n$ . In the uncorrelated case ( $\alpha = 0$ ), the mean system spin energy is always bounded by the two average initial energies. Here, heat always flows from the hot to the cold spins on average. By contrast, for the correlated case ( $\alpha = \sqrt{0.0336}$ ), the



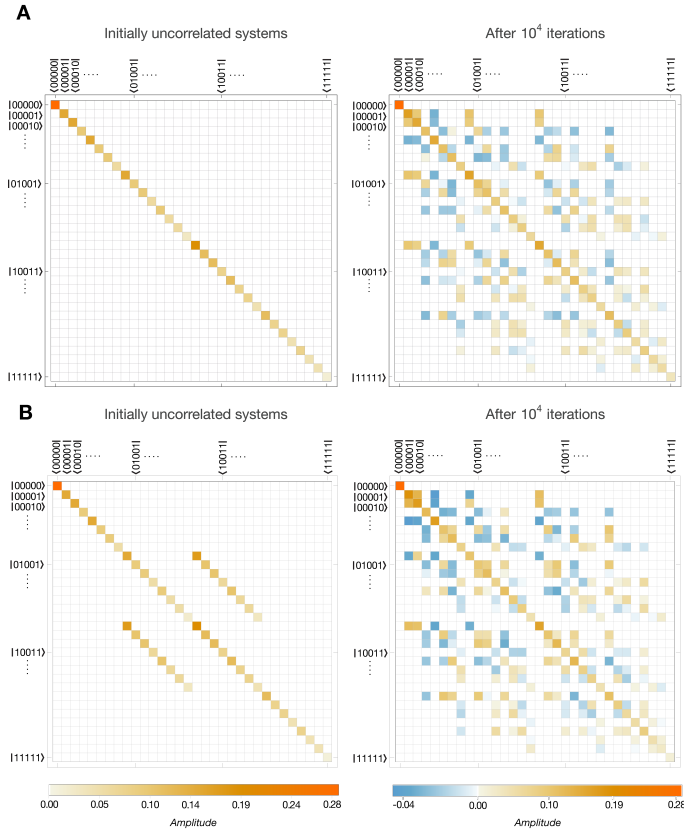


Figure S4. **Evolution of the total density matrix elements.** Numerical simulation of the total density matrix showing thermalization after  $10^4$  steps in the initially uncorrelated (A) and correlated (B) case.

mean system spin energy is seen to cross the red lines (the upper of lower bound of the standard case), revealing a reversal of the arrow of time along the evolution steps.

We may understand how the random interactions induce relaxation by looking to one state of the case  $N = 2$ . We focus on one interaction  $U_{\lambda_2}^{(1,2)}$  between spins 1 and 2 that takes place after one previous interaction  $U_{\lambda_1}^{(0,1)}$  between spins 0 and 1. Since  $|\lambda_1|, |\lambda_2| \ll 1$ , we may apply the Baker-Hausdorff formula to obtain,

$$U_{\lambda_2}^{(1,2)} U_{\lambda_1}^{(0,1)} = \exp(\lambda_1 \mathcal{H}^{(0,1)} + \lambda_2 \mathcal{H}^{(1,2)} + \frac{\lambda_1 \lambda_2}{2} \mathcal{Z}^{(1)} \otimes \mathcal{H}^{(0,2)}), \quad (\text{S6})$$

where  $\mathcal{H}^{(i,j)} = (|01\rangle\langle 10| - |10\rangle\langle 01|)_{(i,j)}$ . Since  $\rho_1$  is not a fully mixed state, the term proportional to  $\mathcal{Z}^{(1)}$  will induce correlations between  $\rho_0$  and  $\rho_2$  due to interference effects. However, as  $N$  increases, the probability that the same pair randomly interacts twice in a row decreases significantly. As a result, a large number of interactions will create an apparent dephasing in the subspace of each pair, at the same time as the total global correlations between all the spins increase, see also Fig. S4.